NANO LETTERS

pubs.acs.org/NanoLett

Measuring Porosity at the Nanoscale by Quantitative Electron Tomography

E. Biermans,[†] L. Molina,[†] K. J. Batenburg,[‡] S. Bals,*[,†] and G. Van Tendeloo[†]

[†]EMAT, University of Antwerp, Groenenborgerlaan 171, B-2020 Antwerp, Belgium, and [‡]Vision Lab, University of Antwerp (CDE), Universiteitsplein 1, B-2610 Wilrijk, Belgium

ABSTRACT Quantitative electron tomography is proposed to characterize porous materials at a nanoscale. To achieve reliable three-dimensional (3D) quantitative information, the influence of missing wedge artifacts and segmentation methods is investigated. We are presenting the "Discrete Algebraic Reconstruction Algorithm" as the most adequate tomography method to measure porosity at the nanoscale. It provides accurate 3D quantitative information, regardless the presence of a missing wedge. As an example, we applied our approach to nanovoids in $La_2Zr_2O_7$ thin films.

KEYWORDS Porous materials, electron tomography, discrete tomography, quantitative

Porous materials form a broad category of solids having different origins and applications. For example, porous media appear in our natural environment and play a fundamental role in earth science and biology. Recently, these materials also became of crucial importance in nanotechnology, where they have applications such as catalysis, separation and energy storage. Independent of the origin of the porous materials, their physical properties largely depend on the structure, density, and distribution of the pores or voids.[1] To control and optimize these parameters, a major step is to measure and characterize them in a reliable manner. At the nanoscale, this can be done using transmission electron microscopy (TEM). Several porous compounds have been studied using this technique in a qualitative manner, but gaining access to quantitative information requires the development of new methodologies. Conventional TEM only provides a two-dimensional (2D) projection of a three-dimensional (3D) object, which prohibits quantitative interpretation. This problem can be overcome by using electron tomography, a technique to create a 3D reconstruction from a series of 2D TEM images collected from the same area of interest under different tilt angles. This technique has been used successfully in many studies on porous materials, but even when 3D reconstructions are obtained, the results are mainly qualitative. This is related to specific problems connected to the technique. For example, in an electron microscope it is often impossible to tilt a sample over 180°, which is mostly due to the limited area for the sample holder in between the objective pole pieces of the microscope. The lack of projections for a range of angles results in a "missing wedge" of information in Fourier space and consequently induces artifacts in the 3D reconstruction.[2−8] These artifacts will hamper a quantitative interpretation of the 3D reconstructed volume. In the present study, we overcome this problem by using a dedicated 360° on-axis rotation tomography holder that is able to acquire a full tilt series without missing wedge. We will show that this is the first important step toward measuring porosity at the nanoscale. Equally important however is the actual quantification of the 3D results. Quantification requires an additional segmentation step after the reconstruction to determine the correspondence between different gray scales in the reconstruction and different compositions in the original structure. It is often neglected that even if projection images can be acquired from a full range of angles, several other types of artifacts will hamper this segmentation step. A quantitative interpretation based on the conventional reconstruction algorithms is therefore quite difficult and is often unreliable. In this paper, we propose a methodology that can be used to quantitatively determine the density of voids or pores in a material. As an example, we will apply our approach to nanovoids in chemical solution derived $La_2Zr_2O_7$ (LZO) oxide thin films,[9] a recently developed intermediate buffer layer for superconducting $YBa_2Cu_3O_{7-\delta}$ (YBCO)-coated conductors for magnet and energy applications. Nanovoids are a typical feature found in such solution derived oxide films processed under a reducing forming gas (Ar-5%H2).[10] They play an important role since they reduce the effective length of matter protecting the metallic substrate from oxidation during the deposition of YBCO.[11]

Experimental Section. The sample used to illustrate our methodology is a LZO oxide thin film that serves as a buffer layer for YBCO-coated conductor technology. This is based on dip-coating a biaxially textured Ni-5 atom %W tape prepared by the RABiTS approach[12] in a precursor solution combined with an annealing treatment. The sample was

* To whom correspondence should be addressed. E-mail: Sara.Bals@ua.ac.be. Tel: +32 3 265 3284. Fax: +32 3 265 3318.

Received for review: 9/8/2010
Published on Web: 11/22/2010

DOI: 10.1021/nl103172r | *Nano Lett.* **2010,** *10,* 5014–5019

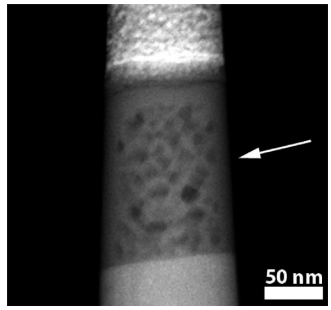

FIGURE 1. HAADF-STEM image of the LZO micropillar sample.

annealed at a temperature of 900 °C and prepared by the chemical solution deposition (CSD) process.[9,13]

Electron tomography tilt series of 2D TEM images are acquired using a Fischione on-axis rotation tomography holder (model 2050). This holder requires a micropillar sample,[14] which is prepared using a FEI Nova Nanolab 200 DualBeam SEM/FIB system. The procedure to prepare these dedicated micropillar samples is explained in more detail in ref 15. Using the dedicated holder, a tilt series is collected over an angular range of ±90° with a 2° increment using high-angular annular dark-field scanning transmission electron microscopy (HAADF-STEM). In HAADF-STEM mode, a HAADF detector will only collect electrons that have been scattered at high angles with respect to the optical axis, resulting in images where the intensity is found to increase monotonically with the thickness of the material, which fulfills the projection requirement for electron tomography.[8] The tilt series is acquired using a JEOL 3000F microscope operated at 300 kV.

After alignment of the 2D projection images using a cross-correlation algorithm in Inspect3D,[16] a 3D reconstruction is carried out using the "Simultaneous Iterative Reconstruction Technique" (SIRT) algorithm as implemented in Inspect 3D. SIRT is often used for electron tomography, but in addition, a novel reconstruction algorithm is used in this study. More details on the use of the so-called "Discrete Algebraic Reconstruction Algorithm" (DART) can be found below and in refs 17 and 18.

Results. A 2D HAADF-STEM projection of the sample is shown in Figure 1. The shape of the micropillar mounted on the tomography holder can be clearly recognized. The LZO layer, indicated by a white arrow, is covered by a Pt layer during the FIB procedure to protect the sample against Ga implantation.

In Figure 1, the voids in the LZO layer can be distinguished as the darker regions, but it is clear that it is impossible to obtain quantitative measurements on porosity from such a 2D projection. Therefore, a tilt series of 2D TEM images is collected and used for 3D reconstruction, which is carried out using the SIRT algorithm. A 3D visualization of the result is presented in Figure 2, together with 2 orthoslices through the 3D reconstruction. The voids are clearly faceted with surfaces oriented parallel with the (111) planes of the LZO material.[10] From such a visualization, valuable information on the shape of the voids can be extracted but quantitative information on the density of the voids is still missing.

To extract quantitative results from the 3D reconstruction, an additional segmentation step is required.[19] During this segmentation step, a correspondence should be made between the different gray levels in the 3D reconstruction and the different compounds of the sample, in this case being LZO and voids. This correspondence is not always straightforward, as can be judged from Figure 2b,c. Therefore, segmentation is generally performed manually but this approach is very time-consuming and even more important, can be subjective. Automatic segmentation by using a threshold at different gray levels might be a method to overcome this problem, but (missing wedge) artifacts can hamper this procedure. Here, we propose to use a threshold, which is specified based on the histogram of the gray levels in the 3D reconstruction (see Figure 3). Two peaks are present corresponding to the voids and LZO. The threshold for segmentation was selected at the onset of the peak corresponding to LZO. In Figure 4, the result of inducing such a threshold is illustrated.

Next, quantification based on segmentation by thresholding is compared to the result obtained by the manual segmentation. Since the same result was obtained by three independent manual segmentations of the data, this result is considered as a reference point in this work. The obtained void densities in the LZO layer are presented in Figure 5, where a comparison is made between a manual segmentation and a segmentation based on thresholding

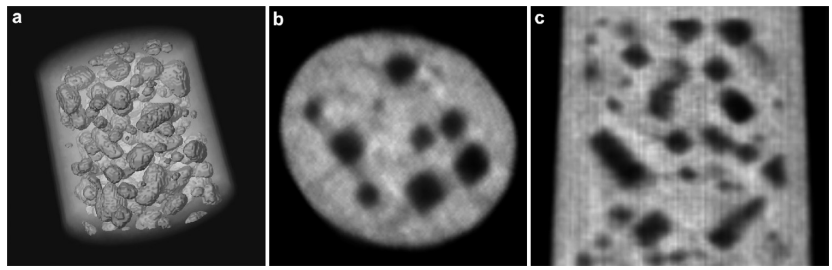

FIGURE 2. (a) Voltex rendering of a 3D reconstruction of a porous $La_2Zr_2O_7$ thin film; (b) *xz*-orthoslice through the 3D reconstruction; (c) *xy*-orthoslice through the 3D reconstruction.

DOI: 10.1021/nl103172r | *Nano Lett.* **2010,** *10,* 5014–5019

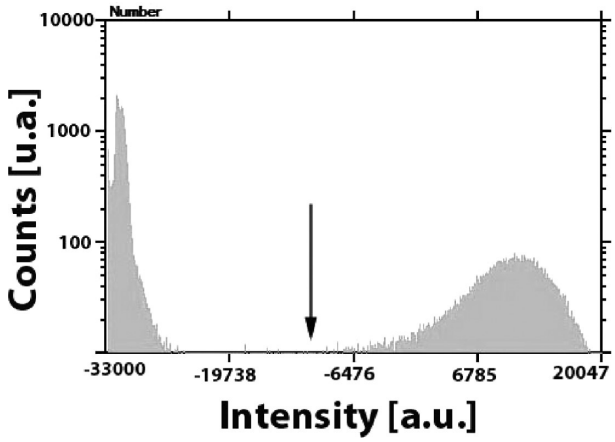

FIGURE 3. Histogram showing the two peaks corresponding the voids and the LZO material. Threshold is selected at the onset of the peak corresponding to LZO (indicated with arrow).

using the same 3D reconstruction, obtained using the SIRT algorithm and based on the series of projection images without missing wedge. From this comparison, a good agreement is found between the manual and the automatic segmentation. Using manual segmentation, the density is determined to be (22.6 ± 2.0)% and by segmentation through thresholding a value of (23.8 ± 2.0)% is found. The fact that we obtain similar results independent of the segmentation method indicates that these measurements can be regarded as reliable. Reference 20 reported nanovoid densities in similar solution derived pyrochlore thin films measured from plan-view TEM images; however, quantification is difficult since information is taken from 2D images. Nanovoid density quantification is improved by electron tomography since the volume of the sample is probed, allowing a true 3D characterization.

Since in most electron tomography studies, the tilt range is limited to about ±70°, it is essential to investigate the effect of the missing wedge on the quantitative information that is extracted. We evaluated the influence of the missing wedge by using only a restricted tilt interval of projection images from the original full tilt series for 3D reconstructions. In this manner, reconstructions are calculated corresponding to (induced) missing wedges of 20°, 40°, and 60°. Orthoslices through these reconstructions are shown in Figure 4 (SIRT algorithm); the effect of the missing wedge is obvious. Elongation of the features and fanning effects, such as described in ref 2 are clearly

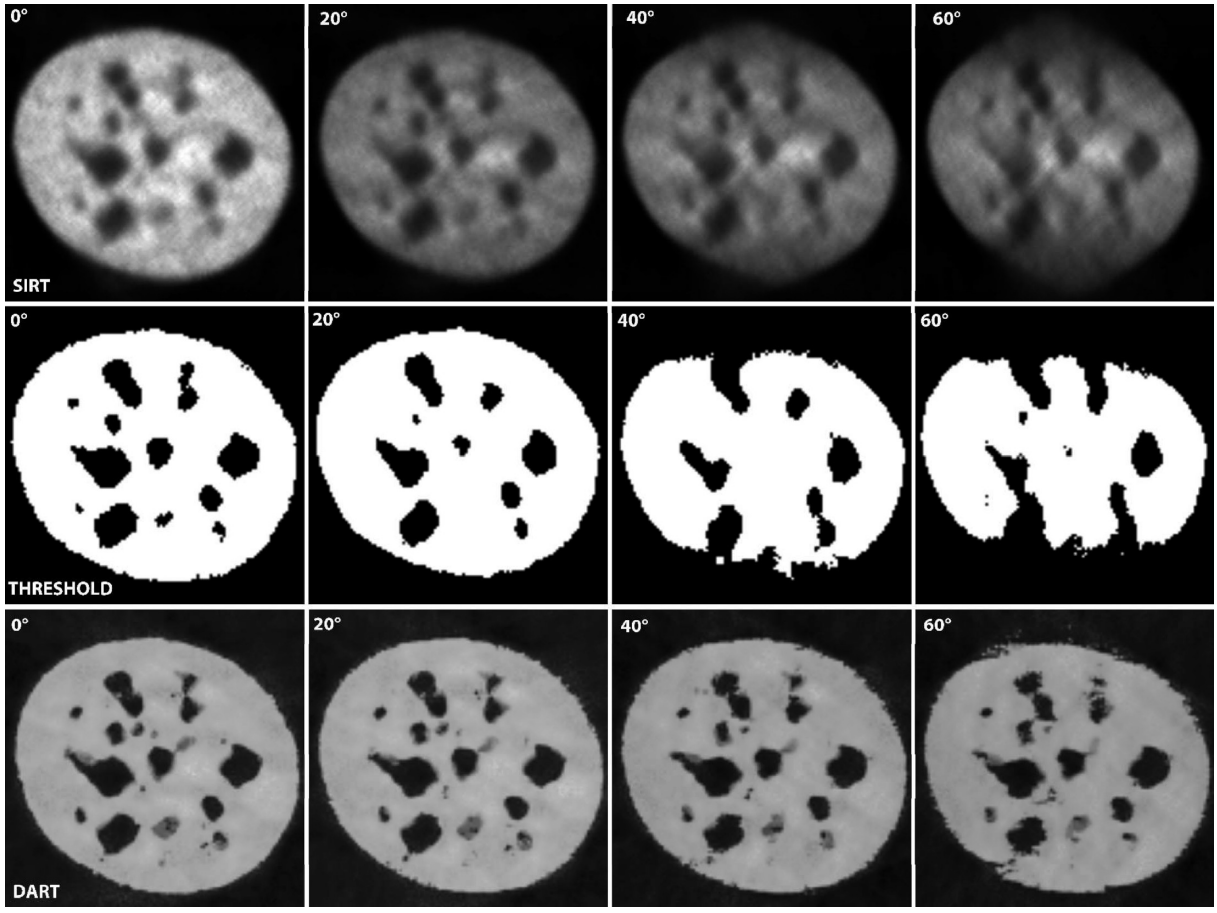

FIGURE 4. Orthoslices through the 3D reconstruction obtained with SIRT, a thresholded SIRT and DART from series with a missing wedge of 0, 20, 40, and 60°.

DOI: 10.1021/nl103172r | *Nano Lett.* **2010,** *10,* 5014–5019

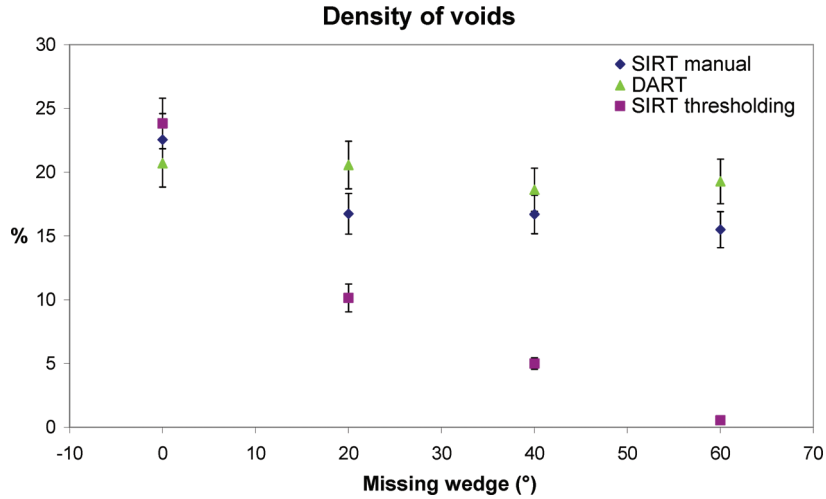

FIGURE 5. Chart showing the density of voids in the LZO layer obtained by manual segmentation of 3D SIRT reconstructions with different values for the missing wedge (SIRT manual), segmentation based on thresholding of 3D SIRT reconstructions (SIRT thresholding), and in situ segmentation in the DART reconstruction (DART).

present. On the basis of these 3D reconstructions, segmentations are again performed manually using the threshold as defined before (Figure 3). The result is illustrated in Figure 4, from which it is obvious that unreliable results are to be expected. This is confirmed quantitatively by the results presented in Figure 5, where both segmentation methods "SIRT + manual segmentation" and "SIRT + segmentation based on threshold" show a significant difference in comparison to the result without missing wedge. Using automatic segmentation, the apparent density of the voids dramatically decreases as a function of increasing missing wedge. For a missing wedge of 40° (which corresponds to a tilt range of ±70°, typical for a tomography experiment), the density of the voids as found by manual segmentation is (16.7 ± 1.5) % whereas using a threshold only (5.0 ± 0.5) % is found. This enormous deviation highlights the influence of the missing wedge when extracting quantitative information on porosity. We therefore conclude that the collection of tilt series without missing wedge is a crucial first step toward quantitative measurements in 3D. Moreover, from our results it is clear that automatic segmentation based on proper thresholding yields reliable quantitative results, but only in the case of a full tilt series of images. This is only possible with a micropillar-shaped sample. Unfortunately, not all porous materials are suitable for preparing a micropillar sample that can be mounted onto the dedicated on-axis tomography holder.

For materials such as powders, another approach should be used. In this respect, the use of discrete tomography, implemented in the DART algorithm is very promising. DART can be used to reconstruct 3D gray scale volumes that contain only a small number of gray levels, typically corresponding to the different materials in the sample. Previous work showed that by using DART, missing wedge artifacts are strongly reduced.[17,18] Additionally, the segmentation is done in situ during the reconstruction, which is very promising for obtaining quantitative results. The power of DART is demonstrated in Figure 4 showing orthoslices through the 3D reconstructions based on this algorithm. A qualitative comparison between the results based on SIRT and DART already indicates that missing wedge artifacts are drastically reduced. To quantify the data, the density of the voids in the LZO layer is also calculated based on the DART reconstruction. The result is shown in Figure 5. The density as found by DART (20.7 ± 1.9) % should be compared to the value of (22.6 ± 2.0) % that is found by manual segmentation. This shows that for a reconstruction based on a full tilt range the density of the voids, as determined by DART, is in good agreement with the result of the SIRT reconstruction. More important however is that, based on the DART reconstruction, the density of the voids does not show a decrease as function of increasing missing wedge as is the case for the segmentation based on thresholding after the SIRT reconstruction. This is not only solid proof that DART is truly able to eliminate missing wedge artifacts, it also demonstrates the reliability of in situ segmentation. It is furthermore important to point out that the use of DART allows one to obtain quantitative results for those samples that can not be prepared in a pillar shape geometry.

Discussion. Quantification in 3D at the nanoscale has been a major challenge in the world of electron tomography over the last couple of years and the number of studies is limited.[21−23] Gaining access to quantitative results is indeed of crucial importance if one wants to determine for example porosity in nanomaterials. In this work, we have demonstrated the importance of collecting 2D projection images over a full tilt range in combination with the use of a reliable segmentation method. Since this segmentation can be done using different approaches, it is relevant to investigate the

DOI: 10.1021/nl103172r | *Nano Lett.* **2010,** *10,* 5014–5019

influence of the segmentation method on the quantitative result. Because of the subjective nature of manual segmentation, it is important to establish objective segmentation procedures, which are preferably automatic. Here, we have compared manual segmentation, segmentation based on thresholding, and in situ segmentation implemented in the DART algorithm.

Figure 4 clearly shows that the different segmentation methods are all in good agreement when they are based on a complete series of 2D projection images. This confirms the reliability of the value found for the density of the voids in the LZO layer in this case. Collecting full range tilt series is obviously of crucial importance when one wants to obtain quantitative results at the nanoscale, such as the local density of pores or voids in porous materials.

As the missing wedge increases, the quality of the 3D reconstruction is expected to become worse. This is indeed reflected in our quantitative data that show a significant decrease of void density both for manual segmentation and thresholding of the SIRT reconstruction. However, the manual segmentation yields significantly better results in comparison to thresholding. On the basis of conventional reconstruction algorithms such as SIRT, reliable results can only be expected when the missing wedge has been completely eliminated. Unfortunately, not all nanostructured samples can be prepared in a pillar shape and in those cases the effect of a missing wedge clearly has to be taken into account. We have shown here that quantitative results can still be obtained by using the DART reconstruction algorithm. Previously we already qualitatively demonstrated that DART results in better quality reconstructions. In addition segmentation is performed in situ during the reconstruction, which is another advantage over SIRT. Here, we have confirmed our previous findings in a quantitative manner. Our results suggest that in case the missing wedge cannot be avoided, which is, for example, the case for nanoporous powders, the porosity can still be determined in a reliable manner using the DART algorithm.

Conclusion. We have demonstrated that quantitative electron tomography is an adequate way to measure porosity at the nanoscale. We have recorded 2D projections without a missing wedge. On the basis of the 3D reconstruction of such series, reliable results on the nanoporosity of a LZO layer are obtained. Whenever a missing wedge cannot be avoided, which is often the case, the use of the DART algorithm for 3D reconstruction is a valid alternative.

Acknowledgment. Authors acknowledge K. Knoth, B. Holzapfel. and O. Eibl for providing a $La_2Zr_2O_7$ buffer layer sample synthesized under the framework and funding of the Virtual Institute "Chemically deposited YBCO superconductors" of the Helmholtz Gemeinschaft. The authors acknowledge financial support from the European Union under the Framework 6 program under a contract for an Integrated Infrastructure Initiative (Reference 026019 ESTEEM). K.J.B. and S.B. are grateful to the Fund for Scientific Research-Flanders, (Contract No. G.0247.08).

REFERENCES AND NOTES

(1) Davis, M. E. Ordered porous materials for emerging applications. *Nature* **2002**, *417* (6891), 813–821.
(2) Weyland, M.; Midgley, P. Electron tomography. *Mater. Today* **2004**, *7* (12), 1.
(3) Koster, A. J.; Ziese, U.; Verkleij, A. J.; Janssen, A. H.; de Jong, K. P. Three-dimensional transmission electron microscopy: A novel imaging and characterization technique with nanometer scale resolution for materials science. *J. Phys. Chem. B* **2000**, *104* (40), 9368–9370.
(4) Sadan, M. B.; Houben, L.; Wolf, S. G.; Enyashin, A.; Seifert, G; Tenne, R.; Urban, K. Bright-Field Electron Tomography of inorganic fullerenes approaching atomic resolution. *Nano Lett.* **2008**, *8* (3), 891–896.
(5) Bals, S.; Van Tendeloo, G.; Kisielowski, C. A new approach for electron tomography: annular dark-field transmission electron microscopy. *Adv. Mater.* **2006**, *18*, 892–895.
(6) Bals, S.; Batenburg, K. J.; Liang, D.; Lebedev, O.; Van Tendeloo, G.; Aerts, A.; Martens, J.; Kirschhock, C. Quantitative three-dimensional modeling of zeotile through discrete electron tomography. *J. Am. Chem. Soc.* **2009**, *131* (13), 4769–4773.
(7) Arslan, I.; Tong, J. R.; Midgley, P. A. Reducing the missing wedge: high-resolution dual axis tomography of inorganic materials. *Ultramicroscopy* **2006**, *106* (11−12), 994–1000.
(8) Midgley, P. A.; Weyland, M. 3D electron microscopy in the physical sciences: the development of Z-contrast and EFTEM tomography. *Ultramicroscopy* **2003**, *96* (3−4), 413–431.
(9) Knoth, K.; Huhne, R.; Oswald, S.; Molina, L.; Eibl, O.; Schultz, L.; Holzapfel, B. Growth of thick chemical solution derived pyrochlore La2Zr2O7 buffer layers for YBa2Cu3O7-x coated conductors. *Thin Solid Films* **2008**, *516* (8), 2099–2108.
(10) Molina, L.; Knoth, K.; Engel, S.; Holzapfel, B.; Eibl, O. Chemically deposited La2Zr2O7 buffer layers for YBCO-coated conductors: film growth and microstructure. *Supercond. Sci. Technol.* **2006**, *19* (11), 1200–1208.
(11) Yu, Z. M.; Odier, P.; Morlens, S.; Chaudouet, P.; Bacia, M.; Zhou, L.; Zhang, P. X.; Jin, L. H.; Li, C. S.; David, P.; Fruchart, O.; Lu, Y. F. Deposition of La2Zr2O7 film by chemical solution deposition. *J. Sol-Gel Sci. Technol.* **2010**, *54* (3), 363–370.
(12) Eickemeyer, J.; Selbmann, D.; Opitz, R.; Wendrock, H.; Maher, E.; Miller, U.; Prusseit, W. Highly cube textured Ni-W-RABiTS tapes for YBCO coated conductors. *Physica C* **2002**, *372*, 814–817.
(13) Molina, L.; Eibl, O.; Knoth, K.; Engel, S.; Huhne, R.; Holzapfel, B. YBCO coated conductors prepared by chemical solution deposition: A TEM study. *Physica C* **2007**, *460*, 1407–1408.
(14) Kato, M.; Kawase, N.; Kaneko, T.; Toh, S.; Matsumura, S.; Jinnai, H. Maximum diameter of the rod-shaped specimen for transmission electron microtomography without the "missing wedge". *Ultramicroscopy* **2008**, *108* (3), 221–229.
(15) Ke, X. X.; Bals, S.; Negreira, A. R.; Hantschel, T.; Bender, H.; Van Tendeloo, G. TEM sample preparation by FIB for carbon nanotube interconnects. *Ultramicroscopy* **2009**, *109* (11), 1353–1359.
(16) Schoenmakers, R. H. M.; Perquin, R. A.; Fliervoet, T. F.; Voorhout, W. Advances in instrumentation and technique-tomography in biological and materials sciences. High resolution, high throughput electron tomography reconstruction. *Microsc. Microanal.* **2005**, *11* (suppl 2), 312–313.
(17) Bals, S.; Batenburg, K. J.; Verbeeck, J.; Sijbers, J.; Van Tendeloo, G. Quantitative three-dimensional reconstruction of catalyst particles for bamboo-like carbon nanotubes. *Nano Lett.* **2007**, *7* (12), 3669–3674.
(18) Batenburg, K. J.; Bals, S.; Sijbers, J.; Kubel, C.; Midgley, P. A.; Hernandez, J. C.; Kaiser, U.; Encina, E. R.; Coronado, E. A.; Van Tendeloo, G. 3D imaging of nanomaterials by discrete tomography. *Ultramicroscopy* **2009**, *109* (6), 730–740.
(19) Weyland, M.; Midgley, P. A. Electron Tomography. In *Nanocharacterisation*; Kirkland, A., Hutchison, J. L., Eds.; Royal Society of Chemistry (RSC) Publishing: Cambridge, U.K., 2007; pp 184−276.

DOI: 10.1021/nl103172r | *Nano Lett.* **2010,** *10,* 5014--5019

(20) Zhao, W. J.; Norman, A.; Phok, S.; Bhattacharya, R. Transmission electron microscope study on electrodeposited Gd2O3 and Gd2Zr2O7 buffer layers for YBa2Cu3O7-delta superconductors. *Physica C* **2008**, *468* (14), 1092–1096.

(21) Midgley, P. A.; Thomas, J. M.; Laffont, L.; Weyland, M.; Raja, R.; Johnson, B. F. G.; Khimyak, T. High-resolution scanning transmission electron tomography and elemental analysis of zeptogram quantities of heterogeneous catalyst. *J. Phys. Chem. B* **2004**, *108* (15), 4590–4592.

(22) Ikeda, Y.; Katoh, A.; Shimanuki, J.; Kohjiya, S. Nano-structural observation of in situ silica in natural rubber matrix by three dimensional transmission electron microscopy. *Macromol. Rapid Commun.* **2004**, *25* (12), 1186–1190.

(23) Kohjiya, S.; Katoh, A.; Shimanuki, J.; Hasegawa, T.; Ikeda, Y. Nano-structural observation of carbon black dispersion in natural rubber matrix by three-dimensional transmission electron microscopy. *J. Mater. Sci.* **2005**, *40* (9−10), 2553–2555.

DOI: 10.1021/nl103172r | *Nano Lett.* **2010,** *10,* 5014--5019